A long-lived swarm on the Central Bransfield Basin, Antarctica

Poli, P[1]., Cabrera, L.[1], Flores, M. C.[2], Báez, J.C.[2], Ammirati, J.B.[3], Vásquez, J. [5] and Ruiz, S.[4]

1 ISTerre Institut des Sciences de la Terre, CNRS, Université Grenoble Alpes, France

2 Centro Sismológico Nacional, Universidad de Chile, Chile.

3 Department of Geology, Faculty of Physics and Mathematics, Universidad de Chile, Chile.

4 Department of Geophysics, Faculty of Physics and Mathematics, Universidad de Chile, Chile.

5 Facultad de Ciencias de la Salud, Universidad de Talca, Región del Maule, Chile

Abstract

We study a large and long-lived earthquakes swarm occurring in 2020-2021 in the Bransfield Basin, south of the South Shetland islands, Antarctica. We make use of local seismological stations to detect and characterize more than 36000 small earthquakes, occurring from the end of August 2020 to June 2021. Together with the occurrence of the ~36000 earthquakes, we observe a significant (up to 8cm) geodetic deformation at nearby GPS stations. By joint interpretation of b-value, spatiotemporal evolution of seismicity and geodetic deformation, we infer a volcanic origin for this swarm, which takes place close to the ridge axis. Our study suggest that a significant amount of extension observed at the Bransfield Basin ridge is occurring in rapid deformation episodes (e.g., 1 year), and is most likely driven by volcanic activity localized at the ridge axial volcanic structure, rather than at the rifting bounding border faults.

Plain language summary

Understanding the extensional tectonic in places at the transition from continental to oceanic spreading, can provide new insights about the extensional processes leading to formation of new oceans. For this scope we study a long-lived (~1 year) swarm of earthquakes occurring in the Bransfield Basin, just to the south of the South Shetland islands, in Antarctica. This basin represents a ridge separating two tectonic plates, and is characterized by extensional tectonic at the transition from rifting to ocean spreading. By detection and characterization of more than 36000 earthquakes and observation of geodetic deformation, we inferred the significant role played by volcanic processes occurring at the ridge axis, in modulating the extension of the basin. This observation differs from purely tectonic extensional processes involving rifting bounding border faults.

Introduction

On August 2020, a significant increment of seismic activity was reported in the Bransfield Basin, south of the South Shetland islands, Antarctica (Fig. 1). Between August 29 and June 2021, the United State Geological Service (USGS, U.S. Geological Survey, 2020) reported ~130 earthquakes with magnitudes larger than 4.0 (Fig. 1). The seismicity was not characterized by any large mainshock (Fig. S1) that could potentially have triggered the prolific occurrence of earthquakes in the region. Similar observations were recently reported by Olivet et al., (2021).

The Central Bransfield Basin is a ridge separating the Antarctic plate (to the South) from the South Shetland microplate (Olivet et al., 2021; Almendros et al., 2020; Taylor et al., 2008 and reference therein, Fig. 1). The NW-SE extension of the ridge results from the combination of slab rollback from the past subduction of the Phoenix microplate under the South Shetland microplate, and transtensional motion between the Scotia and Antarctic plates (Almendros et al., 2020; Taylor et al., 2008; Gràcia et al., 1996). The basin is also characterized by extensive volcanism (Almendros et al., 2020; Taylor et al., 2008), occurring in several submarine structures, as the Orca volcano, located ~20 km southwest from the seismic swarm (Fig. 1, Olivet et al., 2021; Almendros et al., 2020). The Orca Volcano consists of a large caldera surrounded by shallow magma reservoirs (Almendros et al., 2020). The magmatism at Orca volcano is mostly basaltic with mid-ocean ridges characteristics (Barker and Austin, 1998). Significant hydrothermal activity is also observed in the area (Bohrmann et al., 1998). The caldera and shallow magmatic bodies of the Orca volcano, produce a positive magnetic anomaly extending along the axis ridge (Almendros et al., 2020). The 2020-2021 swarm overlaps with the shallow magnetic anomaly located northeast from Orca volcano (Almendros et al., 2020; Olivet et al., 2021). Several other swarms connected with volcanic activity have been observed in the Bransfield Ridge (Almendros et al., 2018, Dziak et al., 2010), but mostly located to the western part of the ridge. No significant earthquakes occurred in the central Bransfield basin since 1970 (Fig. 1).

The Bransfield Ridge is of major geological interest as it represents a back-arc basin at the transition from rifting to ocean spreading (Almendros et al., 2020). We thus analyze in detail the 2020-2021 earthquake sequence to provide new insights about short term processes associated with rifting to spreading evolution, and attempt to distinguish if the swarm, and the related geodetic deformation, are resulting from extensional tectonics or volcanic process (Reiss et al., 2021, Buck et al., 2004, Bergman and Solomon, 1990). To that scope, we make use of the limited data available in the region (Fig. 1). One seismic station (JUBA, network AI) located at the Carlini Base (King George Island, ~20km away from the swarm, Fig. 1) is used to improve the detection of earthquakes using template matching (Gibbons and Ringdal, 2006) and to characterize the waveforms associated which each detected event. We also analyzed data from the nearby GNSS stations (Fig. 1), to assess any deformation associated with the seismic activity. Despite the very limited data available, we were able to characterize the early phase and develop of this largest swarm ever occurred

in the Bransfield Ridge. Our observations seem to support the hypothesis of a volcanic origin of this earthquake sequence.

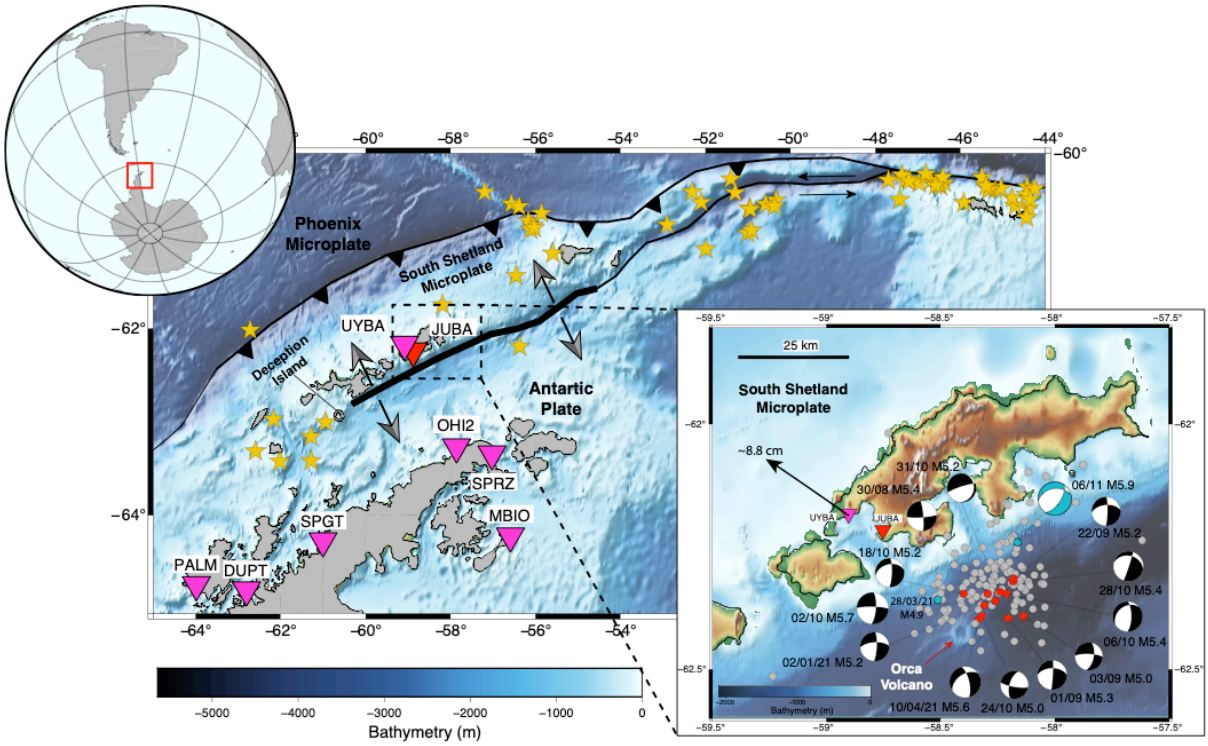

Figure 1: *Red and pink inverted triangles indicate broad-band and GNSS stations used in this study. Yellow stars represent historical seismicity with magnitudes equal or larger than 5.5 from the ISC (International Seismological Centre, 2021) occurred after the eruption of Deception Island (12/08/1970). Right inset: Focal mechanisms (colored compressional quadrants) reported by the USGS since August 28th 2020 and the location of the Orca volcano. The largest event (M 5.9) and another event (M 4.9) indicated in Fig.4 and S4 are highlighted with cyan color. The estimated NW displacement for UYBA respect to the Antarctic plate is indicated with a black arrow (see text for details about GPS processing).*

Data and methodology

2.1 Earthquakes detection and characterization

We use a seismic station located ~20km from the swarm centroid (Fig. 1) to systematically detect and characterize seismic events in the study area. We first downloaded one year (2020 June 1st, to 2021 June 1st) of continuous three-components waveforms recorded at station JUBA. The traces are first band-pass filtered between 1 and 9 Hz to enhance high frequency signals from the local seismicity. Then, we extracted the events corresponding to the USGS catalog

(Fig. 1) within a 12s window (starting 2 s before P-wave arrival), ensuring the presence of both P- and S-waves associated with the swarm events. We visually controlled the quality of each seismogram and manually picked the P- and S-waves on good quality seismograms exhibiting phases well identifiable on the three components. This process yielded 114 earthquakes, the waveforms of which served as templates to scan the continuous data. We then performed the detection of new events with template matching (Gibbons and Ringdal, 2006) and a single station approach (Poli, 2017). Because the use of a single station can reduce the detection sensitivity and increase the presence of unwanted signals, we combined visual inspection and detection with fake templates (e.g., waveforms flipped in time, Cabrera et al., 2020), to define an optimal detection threshold (3-components average correlation coefficient greater than 0.5). This template matching detection, allowed the identification of 36241 earthquakes, ~300 times more than the initial catalogue (Fig. 1). Figure S2 shows examples of detected waveforms.

Then we estimated the magnitude of each newly detected event by computing the mean S-wave amplitude ratio between the template events and the detections over the three components. Using the template event's catalogue magnitude as a reference, the detection magnitude can then be determined assuming that a ratio of 10 corresponds to a variation of one-unit magnitude (e.g., Cabrera et al., 2020).

Figure 2a shows the temporal variations of the seismicity rate. Unlike what can be observed from the initial catalogue, in which the first event occurs on August 29th, 2020, the swarm begins on August 7th, 2020, with a first seismic rate acceleration leading to 1200 events/day on August 29th (Fig. 2a). The rate later decreases with a log-like behavior similar to an Omori law (Omori, 1894), as it is often observed for aftershocks sequences although, no mainshock was observed at the beginning of the sequence. Indeed, the largest event (M = 5.9) occurred on November 6th, 2020 (Fig. S1). The Omori like behavior is thus more likely the result of an external force (e.g., aseismic slip, pore pressure variation) driving the seismicity (e.g., Perfettini and Avouac, 2004; Bourouis and Bernard, 2007). We quantified the seismicity rate decay, by fitting the number of events per day as function of time elapsed from August 29th, 2020 (corresponding to the most active part of the swarm, Fig. 2b). Unlike a classic mainshock-aftershock sequence for which the seismic rate decays proportionally to $1/t^p$, with p=1 (Bourouis and Bernard, 2007), we found a value of p=0.5 which suggests a slower decay. Similar observations (no clear mainshock, slow decay of the Omori-like behavior) were made for the 2014-2015 Deception Island volcanic swarm, in the western part of the Bransfield Basin (Almendros et al., 2018).

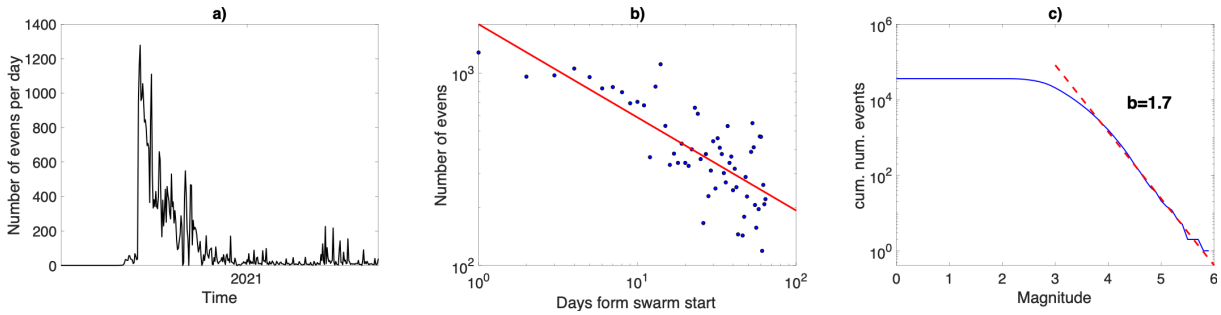

Figure 2: *a) Number of events as function of absolute time. b) Number of events as function of days after August 28th, 2020, plotted with blue dots. The red line shows the regression with p=0.45. c) Cumulative magnitude-frequency distribution for the detected earthquakes. The red dashed line shows the regression for magnitudes ranging from 4 to 6. The corresponding b-value is 1.7.*

To gain more insights about the possible origins of this swarm we also assessed the b-value (Gutenberg and Richter, 1941). For regular earthquake sequence, b-value is usually around 1 (Frohlich and Davis, 1993), and deviation from this average can provide information about stress and/or physical properties of the rock volume (Mogi, 1962; Schorlemmer et al., 2005; Farrel et al., 2009). We use the magnitude frequency distribution of figure 2c to estimate (Wiemer, 2001) a b-value of 1.7±0.1, which is remarkably higher from values characterizing regular earthquake sequences (Frohlich and Davis, 1993; Farrel et al., 2009). Previous studies in this area (Olivet et al., 2021) found a b-value of ~1.2. We believe that the detection of events with much smaller magnitudes allowed us to better resolve the b-value for this swarm. Such a high b-value coincides with other values observed in volcanic areas (e.g., Wilks et al., 2017; Roberts et al., 2015; Farrel et al., 2009).

No clear spatial migration of the seismicity can be observed from the USGS earthquakes locations (fig. S3). However, teleseismic events are usually characterized by significant uncertainties, which could bias this kind of observation. While we could not precisely locate the detected events, due to small events being only visible at JUBA seismic station (Fig. 1), we attempted to discern any spatiotemporal patterns from S-P time analysis, using a single station approach. We first analyzed if any general migration was visible, by plotting the S-P time picked at station JUBA (Fig. 1) when selecting templates (Fig. 3a). No clear global spatial migration was observed but rather some time-limited migration episodes and a shift of the seismicity farther from JUBA starting mid-October 2020 (Fig. 3a).

We also evaluated the relative P- and S-wave travel times for some of the biggest families using templates as reference waveforms, and estimated the delays respect to the reference events by cross correlating 1 second of signal around P and S arrivals. To obtain delays at sub-sample precision, we resampled the data to 100 Hz.

Figure 3b and c shows the results for the largest families, for P and S delays with correlation coefficients larger than 0.7. The seismicity is clustered within a small area, similar to previous volcanic swarms observed in this region (Almendros et al., 2018, Fig. 3). The time delays show short times of coherent delays associated with bursts of seismic events. A possible diffuse migration towards the station can be observed at the beginning of the sequence (Fig. 3b). From analysis of the delay time, we also observed a migration of the seismicity farther from UBYA station (Fig. 3c), in late October, early November 2020, also inferred from S-P time differences (Fig. 3a).

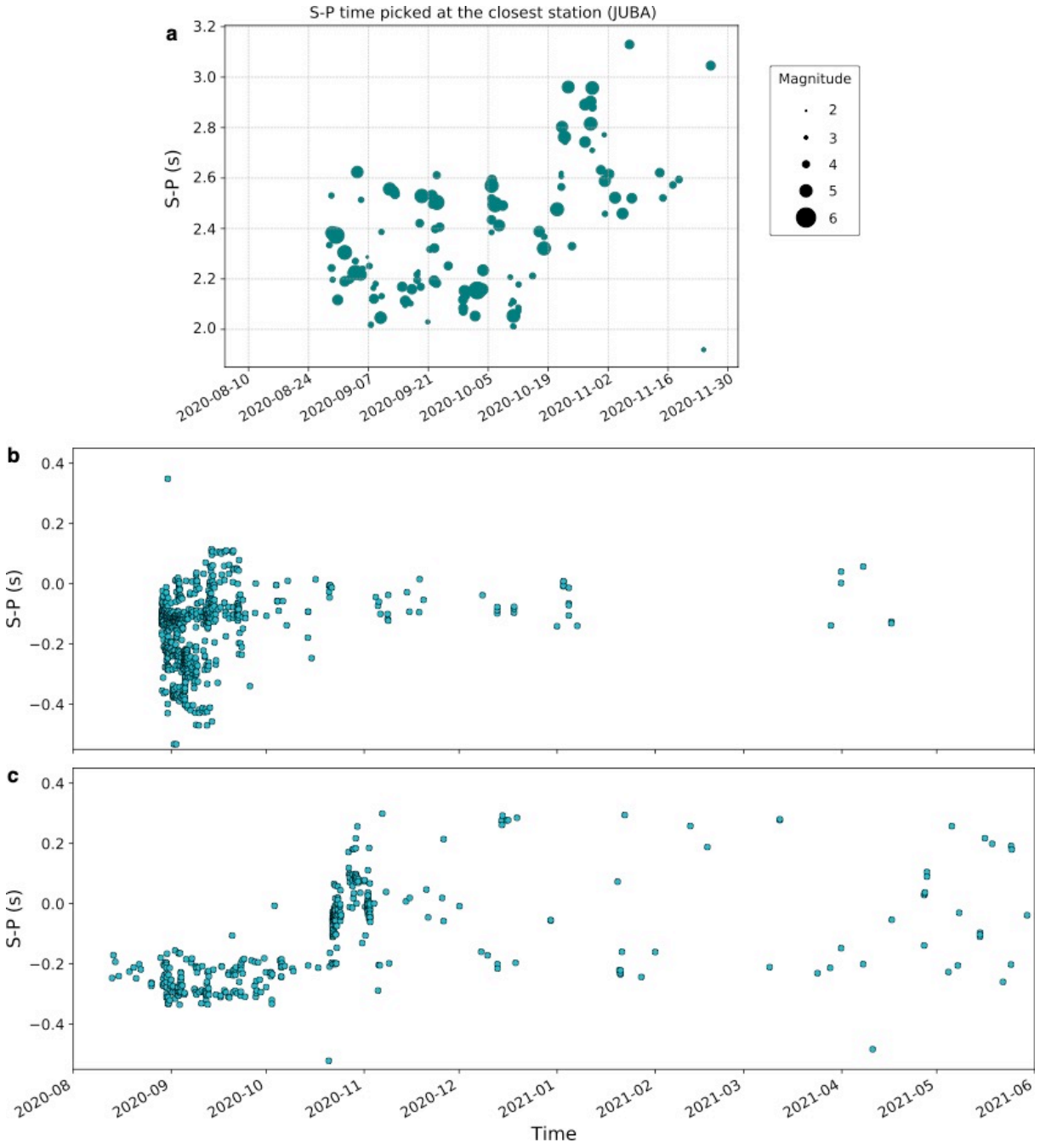

Figure 3: *S-P time from manual picking performed on templates (a) and from delay estimated from cross-correlation of newly detected earthquakes (b-c).*

2.2 Geodetic observations

We use GNSS observations from 2017 up to June 2021, from a set of stations located around the area (Fig. 1). All observations were processed in a network array including several IGS regional stations, applying the differential approach strategy with the Bernese GNSS Software V5.2 (Báez et al., 2018). We stack all daily solutions to generate time series of deformation respect to the Antarctic plate (Fig.4).

The GNSS time series located on the northern zone of Antarctica (UYBA, OHI2, MBIO and SPRZ) show residual deformation consistent with extensional process prior to August 29th 2020 (Fig. 4 a and b). However, no GNSS time series show a clear increase of velocity during the seismicity rate acceleration between August 7th and 28th, 2020 (Fig. 2a, 3c, d, e). The most important velocity change with a clear centimetric displacement (Fig. 1, 4) is be observed from August 28th to June 2021 (when our analysis ends) on both north and east components of station UYBA. The displacement vector is orthogonal to the Bransfield rift axis and is consistent with previous observations from the interseismic period (Taylor et al., 2008). This relative geometry agrees with rift opening dynamics (Almendros et al., 2020, Taylor et al., 2008). The evolution of GNSS displacement at station UYBA during the swarm (Fig. 4c, 4d), closely follows the log-like decrease in cumulative events (Fig. 3), suggesting that both seismicity and surface displacements are driven by the same process (either slow tectonic deformation or volcanic activity).

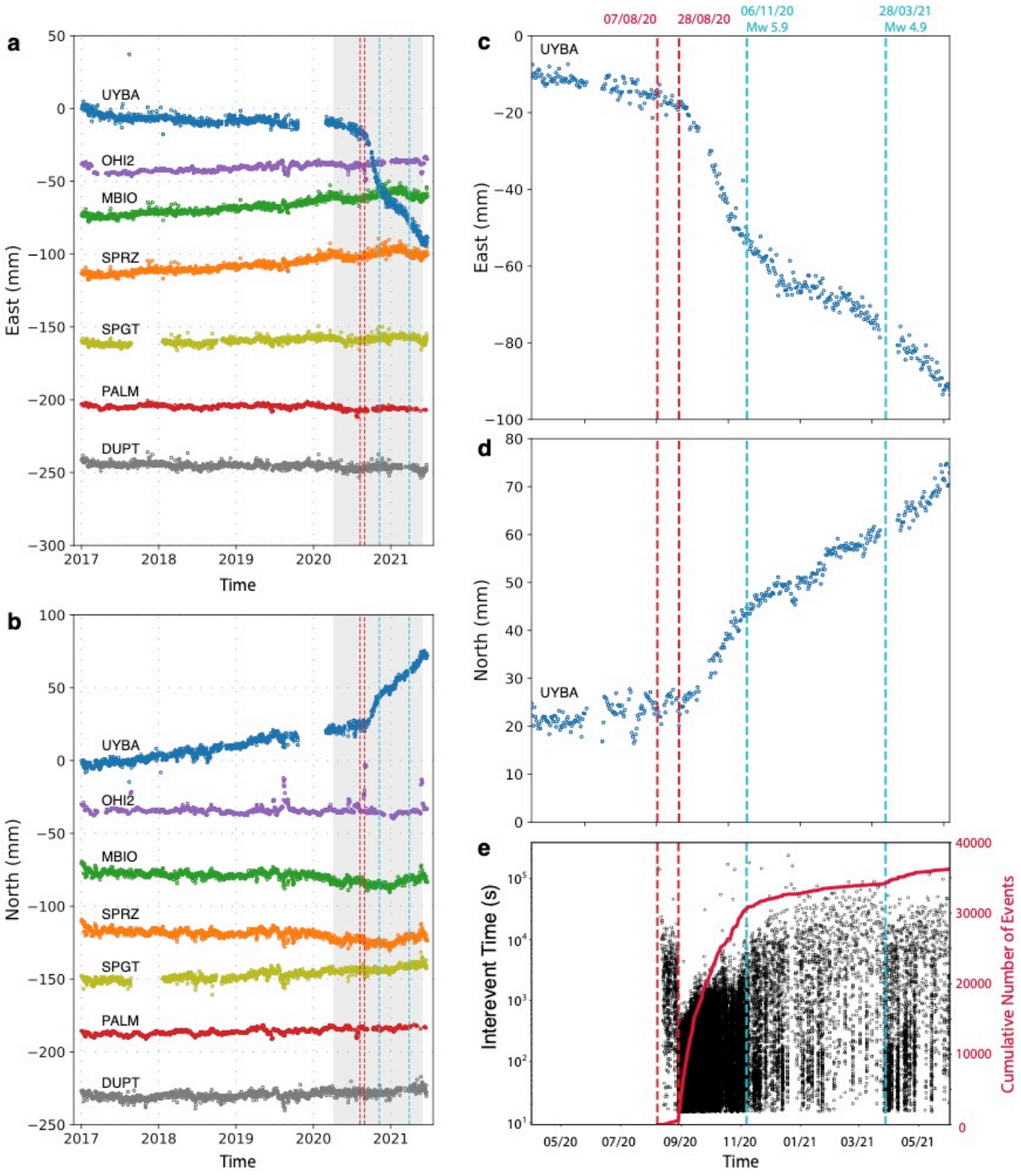

Figure 4: *Detrended GPS displacement at station UBYA (Fig. 1). a) and*

b) are the east and north time series for the full recording time, showing no deformation up to end of august 2020. c) and d) are zooms during the swarm time. e) Cumulative number of events as function of time in red, and recurrence time of events in black dots.

Discussion and conclusions

Despite the lack of dense network of geophysical instruments, we were able to document and characterize the largest swarm ever recorded in the Bransfield Basin (Almendros et al., 2018; Dziak et al., 2010). We detected a long-lived swarm of more than 36000 earthquakes that began on August 7th, 2020, and accelerated on August 29th 2020, challenging previous findings from Olivet et al. (2021). The seismicity rate decreases following a log-like behavior, although no mainshock was observed at the beginning of the swarm (Fig. 2). This observation allows to rule out the mainshock-aftershock mechanism behind the large number of recorded events and observed GNSS deformation (Fig. 4). The cumulative number of earthquakes closely follows the deformation observed at the GNSS station on King George Island (Fig. 1, 4). The orientation of the deformation is orthogonal to the ridge (Fig. 1) and suggests that the ridge spreading is responsible for the 8 cm displacement (Fig. 1, 4). The deformation on King George Island could occur either in response to a dike intrusion (Heimisson and Segall, 2020) or could be associated with a large slow slip events with extensional geometry.

The seismicity is not preceded by any clear mainshock (Fig. S1) and shows a very slow decay in time ($1/t^{0.5}$, fig. 2). Both observations suggest a swarm-like sequence (Mogi, 1963), driven by the deformation processes inferred from the GNSS data (Fig. 4). The estimated b-value is ~1.7, a significantly larger value than previous estimates based a smaller seismicity catalog (Olivet et al., 2021). This large b-value can result from stress heterogeneity, significant thermal gradient and/or presence of magmatic fluids which has been observed in volcanic areas (Farrel et al., 2009).

The spatiotemporal analysis of the seismicity (Fig. 3) resolved with a single station approach, reveals that the swarm nucleated on a small region, with rapid migrations and quick activation of small seismic bursts (Fig. 3). No clear large-scale spatially coherent migration of the seismicity, as the one related to dyke injection discussed by Roman and Cashman (2006) is observed. This behavior can reflect a strong stress heterogeneity (Farrel et al., 2009) also suggested by the high b-value (Fig. 2). We further observe that seismicity mostly lies in a region of high positive magnetic anomaly (Almendros et al., 2020), interpreted as a shallow magmatic body. In addition, most of the large events show strike-slip mechanisms, similar to the swarm model of Hill (1977) and Roman and Cashman (2006). The relatively small number of extensional earthquakes (Fig. 1) suggests that deformation related to rifting (Reiss et al., 2021) is limited during this 2020-2021 long episode.

Taken together, our observations suggest a volcanic origin for the 2020-2021

Bransfield Ridge deformation episode (Bergman and Solomon, 1990). The driving mechanism of the deformation can be either hydrothermal fluids (Reiss et al., 2021) or magma flows (Heimisson and Segall, 2020) at crustal level favored by the presence of conjugate faults (Hill, 1977). The seismicity can also result from local increment of pore fluid pressure (Sibson, 2000). This long-lasting volcanic activity is responsible for the significant deformation inferred from GNSS observations, while seismicity is a by-product of the magmatic activity (Heimisson and Segall, 2020), mainly occurring in limited areas with brittle characteristics and accumulation of stress (Hill, 1977). Our study further illustrates how a significant part of the 7mm/yr extension (Taylor t al., 2008) between the Antarctica Plate and the South Shetland microplate is accommodated in rapid deformation episodes occurring at the ridge axial volcanic structures. Our study also reveals the main role of magmatic structures in favoring the rifting process instead of tectonic deformation occurring in rifting bounding border faults (Reiss et al., 2021, Buck et al., 2004).

Acknowledgements

PP and LC received funding from the European Research Council (ERC) under the

European Union Horizon 2020 Research and Innovation Programme (grant agreements, 802777-MONIFAULTS). JCB was also supported by ANID PIA (ACT192169). SR and JCB were supported by Fondecyt project (N ∘ 1200779, ANID, Chile). JBA is supported by Fondecyt project (Nº 3200633, ANID, Chile). SR thanks to Programa de Riesgo Sísmico (PRS) from University of Chile, Chile. Seismological data are available through the IRIS Data Management Center (IRISDMC) at http://service.iris.edu/fdsnws/dataselect/1/. The corrected GPS time series are at https://www.csn.uchile.cl/red-sismologica-nacional/red-gps/.

BIBLIOGRAPHY

Almendros, J., et al. "BRAVOSEIS: Geophysical investigation of rifting and volcanism in the Bransfield strait, Antarctica." Journal of South American Earth Sciences 104 (2020): 102834.

Almendros, J., et al. "Volcano-Tectonic Activity at Deception Island Volcano Following a Seismic Swarm in the Bransfield Rift (2014–2015)." Geophysical Research Letters 45.10 (2018): 4788-4798.

Báez, J.C.; Leyton, F.; Troncoso, C.; del-Campo, F.; Bevis, M.; Vigny, C.; Moreno, M.; Simons, M.; Kendrick, E.; Brooks, B.; Parra, H.; Blume, F., 2018, the Chilean GNSS network: current status and progress towards early warning applications, SRL, https://doi.org/10.1785/0220180011

Barker, Daniel HN, and James A. Austin Jr. "Rift propagation, detachment faulting, and associated magmatism in Bransfield Strait, Antarctic Peninsula." Journal of Geophysical Research: Solid Earth 103.B10 (1998): 24017-24043.

Bergman, Eric A., and Sean C. Solomon. "Earthquake swarms on the Mid-Atlantic Ridge: Products of magmatism or extensional tectonics?." Journal of Geophysical Research: Solid Earth 95.B4 (1990): 4943-4965.

Bohrmann, Gerhard, et al. "Hydrothermal activity at Hook Ridge in the central Bransfield basin, Antarctica." Geo-Marine Letters18.4 (1998): 277-284.

Bourouis, Seid, and Pascal Bernard. "Evidence for coupled seismic and aseismic fault slip during water injection in the geothermal site of Soultz (France), and implications for seismogenic transients." Geophysical Journal International 169.2 (2007): 723-732.

Buck, W. Roger. "1. Consequences of Asthenospheric Variability on Continental Rifting." Rheology and deformation of the lithosphere at continental margins. Columbia University Press, 2004. 1-30.

Cabrera, L., Poli, P., & Frank, W. B. (2020, December). A Clustered Preparatory Phase of the 2009 Mw 6.3 L'Aquila Earthquake. In *AGU Fall Meeting Abstracts* (Vol. 2020, pp. S029-0002).

Dziak, Robert P., et al. "Tectonomagmatic activity and ice dynamics in the Bransfield Strait back-arc basin, Antarctica." Journal of Geophysical Research: Solid Earth 115.B1 (2010).

Farrell, Jamie, Stephan Husen, and Robert B. Smith. "Earthquake swarm and b-value characterization of the Yellowstone volcano-tectonic system." Journal of Volcanology and Geothermal Research 188.1-3 (2009): 260-276.

Frohlich, Cliff, and Scott D. Davis. "Teleseismic b values; or, much ado about 1.0." Journal of Geophysical Research: Solid Earth 98.B1 (1993): 631-644.

Gibbons, Steven J., and Frode Ringdal. "The detection of low magnitude seismic events using array-based waveform correlation." Geophysical Journal International 165.1 (2006): 149-166.

Gràcia, Eulàlia, et al. "Morphostructure and evolution of the central and eastern Bransfield basins (NW Antarctic Peninsula)." Marine Geophysical Researches 18.2-4 (1996): 429-448.

Gutenberg, Beno, and Charles Richter. Seismicity of the Earth. Vol. 34. Geological Society of America, 1941.

Heimisson, Elías R., and Paul Segall. "Physically Consistent Modeling of Dike-Induced Deformation and Seismicity: Application to the 2014 Bárðarbunga Dike, Iceland." Journal of Geophysical Research: Solid Earth 125.2 (2020): e2019JB018141.

Hill, David P. "A model for earthquake swarms." Journal of Geophysical Research 82.8 (1977): 1347-1352.

International Seismological Centre (2021), On-line Bulletin, https://doi.org/10.31905/D808B830

Mogi, Kiyoo, Magnitude–frequency relation for elastic shocks accompanying fractures of various materials and some related problems in earthquakes

Bull. Earthq. Res. Inst. Univ. Tokyo, 40 (1962), pp. 831-853

Mogi, Kiyoo. "Some discussions on aftershocks, foreshocks and earthquake swarms: the fracture of a semi-infinite body caused by an inner stress origin and its relation to the earthquake phenomena (third paper)." = Bulletin of the Earthquake Research Institute, University of Tokyo 41.3 (1963): 615-658.

Olivet, Judith Loureiro, et al. "A seismic swarm at the Bransfield Rift, Antarctica." Journal of South American Earth Sciences(2021): 103412.

Omori, F., On the aftershocks of earthquake, J. Coll. Sci., Imp. Univ. Tokyo, 1894, vol. 7, pp. 111–200.

Perfettini, H., and J-P. Avouac. "Postseismic relaxation driven by brittle creep: A possible mechanism to reconcile geodetic measurements and the decay rate of aftershocks, application to the Chi-Chi earthquake, Taiwan." Journal of Geophysical Research: Solid Earth 109.B2 (2004).

Poli, Piero. "Creep and slip: Seismic precursors to the Nuugaatsiaq landslide (Greenland)." Geophysical Research Letters 44.17 (2017): 8832-8836.

Reiss, M. C., et al. "The impact of complex volcanic plumbing on the nature of seismicity in the developing magmatic natron rift, tanzania. front." Earth Sci 8 (2021): 609805.

Roberts, Nick S., Andrew F. Bell, and Ian G. Main. "Are volcanic seismic b-values high, and if so when?." Journal of Volcanology and Geothermal Research 308 (2015): 127-141.

Roman, Diana C., and Katharine V. Cashman. "The origin of volcano-tectonic earthquake swarms." Geology 34.6 (2006): 457-460.

D. Schorlemmer, S. Wiemer, M. Wyss, Variations in earthquake-size distribution across different stress regimes, Nature, 437 (2005), pp. 539-542

Sibson, Richard H. "Fluid involvement in normal faulting." Journal of Geodynamics 29.3-5 (2000): 469-499.

Taylor, Frederick W., et al. "Kinematics and segmentation of the South Shetland Islands-Bransfield basin system, northern Antarctic Peninsula." Geochemistry, Geophysics, Geosystems9.4 (2008).

U.S. Geological Survey, 2020, Earthquake Lists, Maps, and Statistics, accessed March 18, 2020 at URL https://www.usgs.gov/natural-hazards/earthquake-hazards/lists-maps-and-statistics

Wiemer, Stefan. "A software package to analyze seismicity: ZMAP." Seismological Research Letters 72.3 (2001): 373-382.

Wilks, Matthew, et al. "Seismicity associated with magmatism, faulting and hydrothermal circulation at Aluto Volcano, Main Ethiopian Rift." Journal of Volcanology and Geothermal Research 340 (2017): 52-67.

Supplementary material

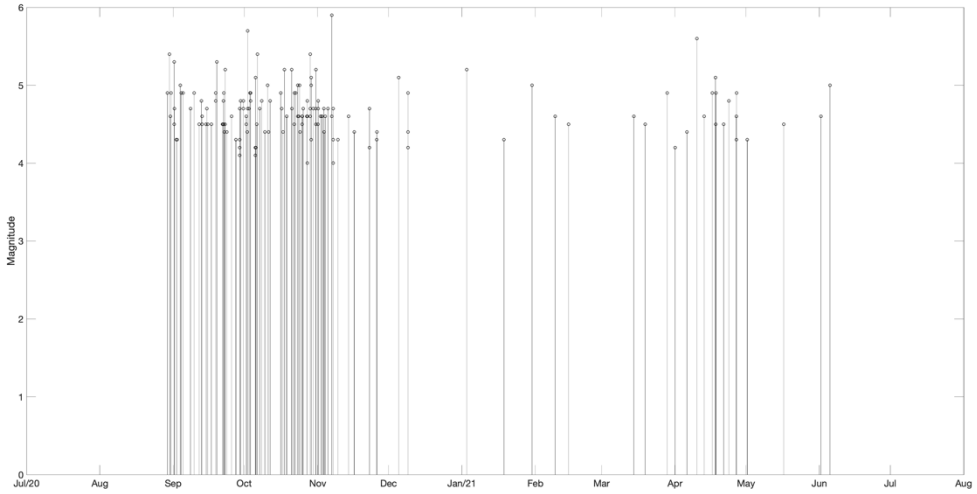

Figure S1: Time evolution of magnitude for the 114 events in the USGS catalogue.

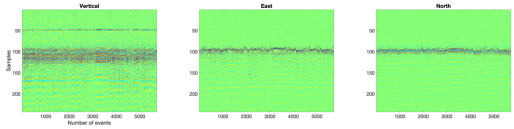

Figure S2: Example of detected waveforms with singe station template matching for three components.

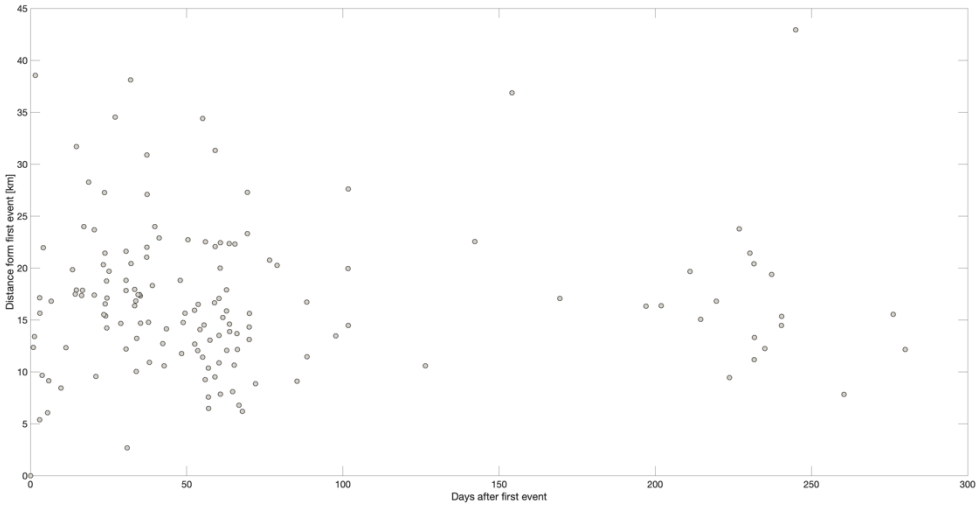

Figure S3: Distance respect to the first event of the sequence as function of time, for events in the USGS catalog.